VIP Superconductivity

DOI: 10.1002/anie.201102866

# Recovery of a Parentlike State in $Ba_{1-x}K_xFe_{1.86}Co_{0.14}As_2$**

*Veronika Zinth, Til Dellmann, Hans-Henning Klauss, and Dirk Johrendt**

*Dedicated to Peter Klüfers on the occasion of his 60th birthday*

Superconductivity in iron-based materials with critical temperatures $T_c$ up to 55 K emerges from layers of edge-sharing $FeX_{4/4}$-tetrahedra, where $X$ is either a pnictide or chalcogenide.[1–5] Several structure types that contain superconducting phases were identified, mostly derivatives of the *anti*-PbFCl and $ThCr_2Si_2$ type.[6] Some are stoichiometric superconductors like LaOFeP, LiFeAs, or FeSe,[7–9] but others like LaOFeAs, $BaFe_2As_2$, or NaFeAs are initially antiferromagnetic metals.[10–13] These so-called parent compounds become superconductors if the charge of the $(FeAs)^{\delta-}$ layer is modified by chemical substitution. The latter is referred to as electron or hole doping, even though charges are varied up to $\pm 0.2\,e^-$/FeAs, which is two orders of magnitude more than in semiconductors, where the term doping has its origin. Keeping this sophistry in mind, we use the term conveniently.

It is accepted that doping of the metallic iron arsenides sensitively tunes the Fermi surface into a state that favors superconductivity.[14] Even though the true nature of this state appears less clear than ever,[15] it is undisputed that the electronic situation of the undoped iron arsenides LaOFeAs and $BaFe_2As_2$ is unstable owing to Fermi surface nesting.[16] Hole- and electronlike cylinders are connected in momentum space by the antiferromagnetic wave vector $(\pi,\pi)$.[17] As long as this nesting is good, the systems undergo structural and magnetic phase transitions to slightly distorted crystal structures with antiferromagnetic ordering at low temperatures. But charge doping shifts the chemical potential away from good nesting until the phase transitions are finally suppressed. Experiments[17,18] and theoretical investigations[19,20] suggest that strong interband scattering between nearly nested Fermi surface sheets plays an important role in superconductivity. In this scenario, the pairing strength (and hence the $T_c$) depends on the enhancement of the spin susceptibility at a nearly nested wave vector.[21]

$BaFe_2As_2$ with the tetragonal $ThCr_2Si_2$-type structure turned out to be exceedingly flexible with respect to substitution. Hole doping was first realized by substitution of barium with potassium ($\rightarrow Ba_{1-x}K_xFe_2As_2$),[3,22] and electron doping by exchanging cobalt for iron ($\rightarrow BaFe_{2-x}Co_xAs_2$).[23] Both phase diagrams are compiled in Figure 1. With hole doping, the onset of superconductivity is at about $-0.05\,e^-$/FeAs, and the highest $T_c$ is 38 K at $-0.2\,e^-$/FeAs, while by electron doping the onset is at $+0.03\,e^-$ and the highest $T_c$ is 25 K at $+0.07\,e^-$/FeAs. Furthermore, the superconducting dome spans $0.45\,e^-$ by hole doping but only $0.11\,e^-$ in the case of electron doping.

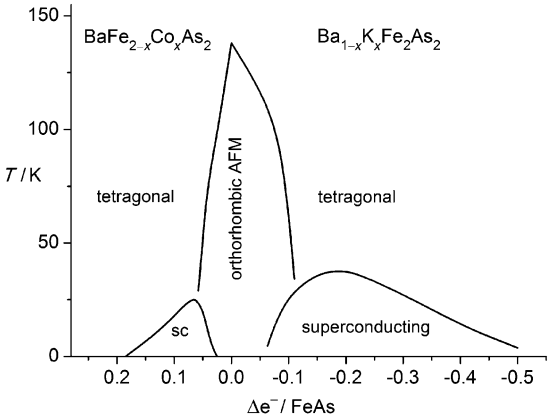


***Figure 1.*** Phase diagrams of hole- and electron-doped $BaFe_2As_2$. Data from Refs. [21] and [23]. AFM = antiferromagnetic metal, sc = superconducting.

This asymmetry may indicate that excess positive or negative charges act differently on the electronic system of $BaFe_2As_2$, but the true relationships are not clear. A DFT study of the cobalt-doped system suggests that the extra electron remains located at the cobalt atom, which acts as scattering center only.[25] Recent photoemission results also indicate filling of rigid bands by doping.[26] However, the direct comparison of electron and hole doping is flawed by the fact that cobalt substitution adds disorder into the FeAs plane where superconductivity emerges, while the layers remain clean by hole doping with potassium at the barium site. Unfortunately, substitutions with electron-poorer 3d metals (Mn, Cr) do not induce superconductivity.[27] Electron doping was also achieved in $Sr_{1-x}La_xFe_2As_2$, giving critical temperatures up to 22 K,[28] but the sample quality still allows no clear relation between the La concentration and $T_c$.

To shed more light on the effect of charge modifications in the $(FeAs)^{\delta-}$ layers of $BaFe_2As_2$, we studied the solid solution $Ba_{1-x}K_xFe_{1.86}Co_{0.14}As_2$. Thus we gradually compensate the optimal electron doping in $BaFe_{1.86}Co_{0.14}As_2$ by holes created by additional potassium substitution. The effects on the

[*] V. Zinth, Prof. Dr. D. Johrendt
Department Chemie, Ludwig-Maximilians-Universität München
Butenandtstrasse 5–13 (Haus D), 81377 München (Germany)
E-mail: johrendt@lmu.de
T. Dellmann, Prof. Dr. H.-H. Klauss
Institut für Festkörperphysik, Technische Universität Dresden
Helmholtzstrasse 10, 01069 Dresden (Germany)

[**] This work was financially supported by the German Research Foundation (DFG) within the priority program SPP1458, projects JO257/6-1 and KL1086/10-1.

Supporting information for this article is available on the WWW under http://dx.doi.org/10.1002/anie.201102866.

crystal structure, superconductivity, and magnetism are determined and discussed herein.

Phase homogeneity and crystal structure parameters were determined by Rietveld refinements of X-ray powder patterns. A typical example is shown in Figure 2. The structure is

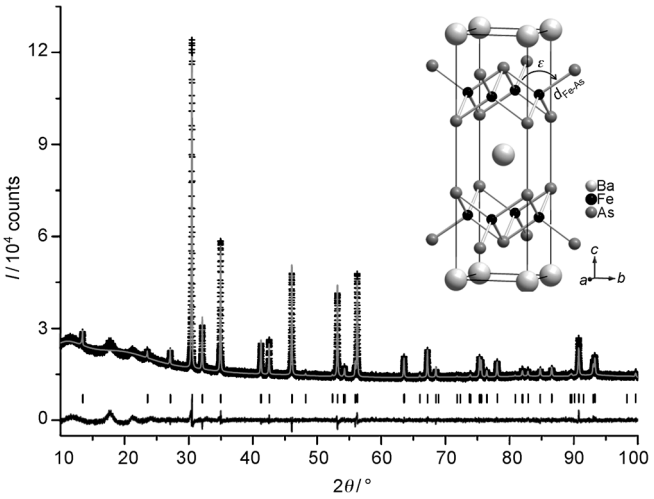


***Figure 2.*** X-ray powder pattern (top, black), Rietveld fit (top, gray) and difference curve (bottom) of $Ba_{1-x}K_xFe_{1.86}Co_{0.14}As_2$ ($x=0.2$). Inset: Crystal structure with Fe–As bond length $d_{Fe\text{-}As}$ and bond angle $\varepsilon$.

completely described by the lattice parameters and the $z$ coordinate of arsenic at the 4*e* site (0,0,$z$) that determines the Fe–As bond length ($d_{Fe\text{-}As}$) and the As-Fe-As bond angle $\varepsilon$ (inset in Figure 2). In $Ba_{1-x}K_xFe_{1.86}Co_{0.14}As_2$, the lattice parameters $a$ and $c$ vary linearly with the potassium concentration, similar to the case for cobalt-free $Ba_{1-x}K_xFe_2As_2$.

Figure 3 shows the normalized changes of the structure parameters versus the variation of the electron count $\Delta e^-$ per FeAs layer. Lines are fits to the literature data of electron-doped $BaFe_{2-x}Co_xAs_2$[24] and hole-doped $Ba_{1-x}K_xFe_2As_2$.[22] We find an almost exact coincidence of all parameters in the hole-doped area. The lattice parameters in the electron-doped area do not agree with those of $BaFe_{2-x}Co_xAs_2$, but continue increasing ($a$) and decreasing ($c$) and rather follow the lines of the potassium-substituted compounds extrapolated into the electron-doped area. The Fe–As bond lengths and As-Fe-As bond angles are close to the expected values in the electron-doped area, but the changes are very small and the extrapolations from the hole-doped part are also close to the fits for electron doping. From these data we conclude that the crystal structure is mainly dominated by the potassium substitution in terms of atom size requirements. The increased charge alone cannot recover the crystal structures of electron-doped $BaFe_{2-x}Co_xAs_2$ in $Ba_{1-x}K_xFe_{1.86}Co_{0.14}As_2$.

The undoped parent compound $BaFe_2As_2$ undergoes a structural and magnetic phase transition at 140 K.[12] We checked our samples for the orthorhombic distortion by structure determinations at low temperatures. The results are depicted in Figure 4. The transition is absent in $BaFe_{1.86}Co_{0.14}As_2$ ($x=0$), as known from the literature.[23] When the electron doping becomes gradually compensated

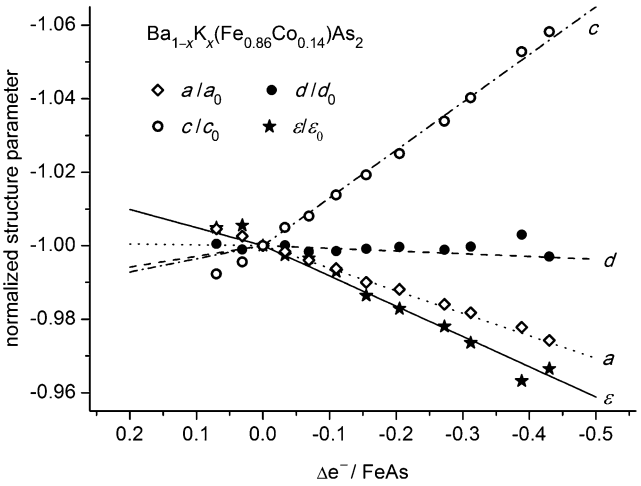


***Figure 3.*** Normalized structure parameters (lattice parameters $a$, $c$, Fe–As bond length $d$, As-Fe-As angle $\varepsilon$) of $Ba_{1-x}K_xFe_{1.86}Co_{0.14}As_2$ plotted against the electron transfer per FeAs. Lines are fits to literature data of $BaFe_{2-x}Co_xAs_2$[24] and $Ba_{1-x}K_xFe_2As_2$.[22]

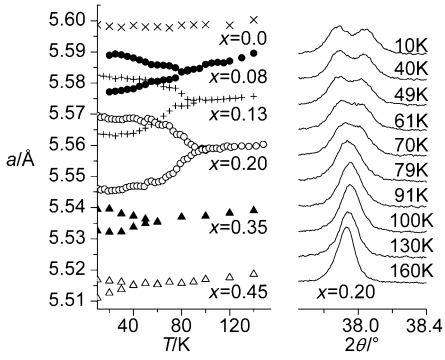


***Figure 4.*** Left: Orthorhombic distortion of $Ba_{1-x}K_xFe_{1.86}Co_{0.14}As_2$ at low temperatures. Right: Temperature dependence of the (110) reflection in $Ba_{1-x}K_xFe_{1.86}Co_{0.14}As_2$ with $x=0.2$.

by potassium doping, we again observe the splitting of the lattice parameters that indicates the structural transition. The effect becomes stronger and shifts to higher temperatures up to the nominal potassium concentration of $x=0.2$, at which the electron doping has just been completely compensated. With further increased hole doping, the distortion becomes smaller again and is finally absent at $x>0.5$. This result emphasizes the important effect of the charge concentration on the structural instability, which has its origin in the nested Fermi surface. As soon as we restore the charge balance, and thus the nesting condition, the instability returns immediately, despite the structural disorder induced by the simultaneous doping at the iron and barium sites.

The recovered structural transition of compound $Ba_{1-x}K_xFe_{0.86}Co_{0.14}As_2$ at $x=0.2$ is accompanied by antiferromagnetic ordering as known from the parent compound $BaFe_2As_2$.[12] Figure 5 shows temperature-dependent $^{57}Fe$ Mössbauer spectra of $Ba_{0.8}K_{0.2}Fe_{1.86}Co_{0.14}As_2$. The single absorption line is subject to magnetic hyperfine field splitting at low temperatures that proves static magnetic ordering. The magnetic order parameter (inset in Figure 5) shows the onset

  

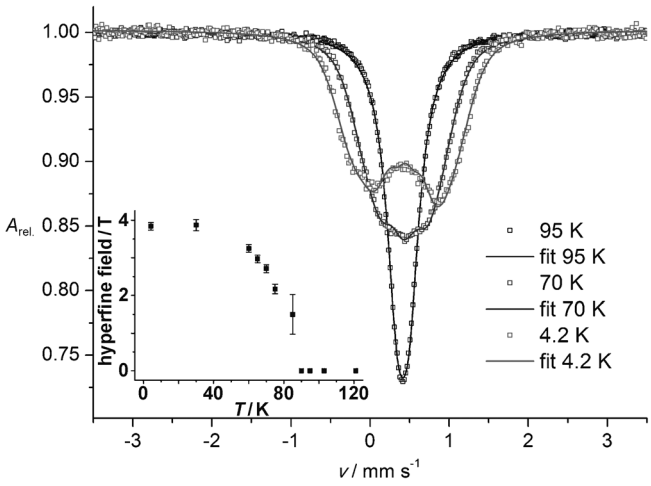


***Figure 5.*** $^{57}$Fe Mössbauer spectra of $Ba_{0.8}K_{0.2}Fe_{1.86}Co_{0.14}As_2$. The inset shows the temperature dependence of the magnetic hyperfine field.

at about 85 K, close to the splitting of the lattice parameters at about 92 K (Figure 4). The hyperfine field converges at 3.9 T at low temperatures, which is smaller than the value of 5.7 T measured in $BaFe_2As_2$.[12] Since the orthorhombic splitting is also reduced in comparison to $BaFe_2As_2$, the strong correlation between magnetic and structural order parameters generally observed in the Ba- and Sr-based iron pnictides with $ThCr_2Si_2$ structure is maintained.[29]

Figure 6 shows the resistivity and alternating-current (AC) volume susceptibility plots. $BaFe_{1.86}Co_{0.14}As_2$ ($x=0$) is superconducting below 25 K, as reported in the literature.[24] Potassium doping decreases the critical temperature to 23 K at $x=0.08$ until superconductivity is absent in the samples with $x=0.13$ and 0.2, where the excess electrons are compensated by the holes introduced by potassium substitution. When the hole doping outweighs electron doping in the samples with $x>0.25$, superconductivity appears again and reaches the highest $T_c$ of 28.6 K at $x=0.45$. Thus the

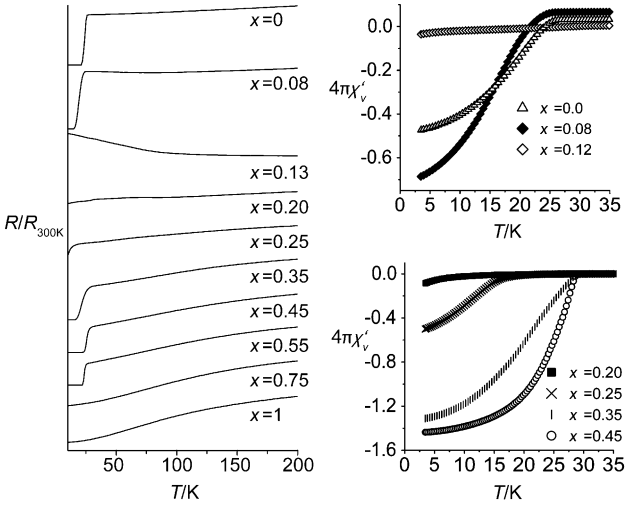


***Figure 6.*** Normalized electrical resistances ($R/R_{300K}$) and AC volume susceptibilities $\chi'_v$ of $Ba_{1-x}K_xFe_{1.86}Co_{0.14}As_2$ samples.

emergence of superconductivity is controlled by the charge concentration and shows the same behavior as known from the only-cobalt- and only-potassium-substituted systems, but with smaller $T_c$ in the hole-doped domain. Furthermore, the ordered magnetic moment and the orthorhombicity parameter $\delta_o=(a-b)/(a+b)$ near the compensated concentration are smaller than in $BaFe_2As_2$. The phase diagram that arises from our data is presented in Figure 7. We note that the series $Ba_{1-x}K_x(Fe_{1-y}Co_y)_2As_2$ has been published recently by Suzuki et al.,[30] but their diagram has no data points in the range that is of interest here.

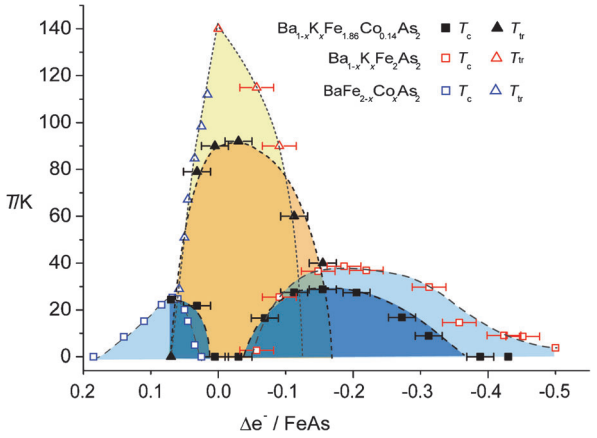


***Figure 7.*** Phase diagram of $Ba_{1-x}K_xFe_{1.86}Co_{0.14}As_2$ (dark blue/orange) compared to the phase diagrams of $Ba_{1-x}K_xFe_2As_2$ and $BaFe_{2-x}Co_xAs_2$ (light blue/yellow). $T_{tr}$ = structural transition temperature.

The phase diagram of $Ba_{1-x}K_xFe_{1.86}Co_{0.14}As_2$ combines those of $Ba_{1-x}K_xFe_2As_2$ ($x=0$–1) and $BaFe_{2-x}Co_xAs_2$ ($x=0$–0.185) by varying only one parameter. The superconducting domes (dark blue shaded areas in Figure 7) are similar to those of the only-cobalt- and only-potassium-doped phases (light blue), and the areas of the orthorhombically distorted magnetic parentlike phases (orange and yellow) are also comparable. The lower phase-transition temperatures and magnetic moments of the charge-compensated phases around $\Delta e^-=0$ may be due to the disorder induced by the cobalt substitution in the iron layer. This disorder could also be the reason for the lower $T_c$ in the hole-doped area and the earlier vanishing of superconductivity at $-0.38\,e^-$.

Our results show that the charge concentration is the crucial parameter that controls magnetism, lattice distortion, and the onset of superconductivity in electron- and hole-doped $BaFe_2As_2$. Especially the onset of superconductivity at the same hole concentration as in the cobalt-free phase ($-0.05\,e^-$) is striking and underlines the impact of the charge. The crystal structure itself in terms of lattice parameters, Fe–As bond lengths, and bond angles appear to be less affected by the charge variation, but rather controlled by atom size requirements. The latter is most obvious for the $c$ axis, which shrinks much more strongly with electron doping ($\Delta e^-=$ 0–0.1) by decreasing the potassium content in $Ba_{1-x}K_xFe_{0.86}Co_{0.14}As_2$ than in $BaFe_{2-x}Co_xAs_2$ (Figure 3).

  

Our results are also in good agreement with the photoemission data, suggesting a rigid-band-like filling or depleting of the electronic states near the Fermi level.[26]

Even though the occurrence of superconductivity is clearly connected to the charge of the $(FeAs)^{\delta-}$ layer, the role of the crystal structure should not be underestimated. We noticed early on that the maximum $T_c$ of 38 K in $Ba_{1-x}K_xFe_2As_2$ at $x \approx 0.4$ ($\Delta e^- \approx -0.2$) coincides with an As-Fe-As bond angle close to the ideal value of 109.47°.[22] Subsequently collected data demonstrated this correlation for many other iron-based superconductors.[31] Our samples show the maximum $T_c$ at $\Delta e^- = -0.16$ when the angle is 109.5°, slightly shifted from the cobalt-free phases that have the maximum at $\Delta e^- = -0.2$ (Figure 7).

In spite of the apparent relation to $T_c$, the true role of the bond angle is still unclear. Even its decrease from 111.1° in $BaFe_2As_2$ to 109.5° and lower by hole doping cannot be well understood from atom sizes alone, because substitution of alkaline metals for barium always decreases the angle. Even if barium is replaced by much smaller sodium atoms in $Ba_{1-x}Na_xFe_2As_2$,[32] the *c* axis increases and the angle becomes smaller until it reaches 109.5° at $x \approx 0.4$, where again $T_c$ is the highest. This situation indicates that the angle may also be controlled by the electron count.

In summary, we have shown how the physical properties of doped $BaFe_2As_2$ are predominantly controlled by the charge of the $(FeAs)^{\delta-}$ layers. Continuous adjustment from electron to hole doping in the solid solution $Ba_{1-x}K_xFe_{1.86}Co_{0.14}As_2$ tunes the system from superconductivity to a magnetic state and back to superconductivity. This recovery of the magnetic phase similar to that of the parent compound is unprecedented and emphasizes the role of the layer charge. Our results suggest that structural parameters like bond length or angles play a minor role with respect to the incurrence of superconductivity in electron- or hole-doped systems but are certainly important to achieve the highest possible critical temperatures.

## Experimental Section

$Ba_{1-x}K_xFe_{1.86}Co_{0.14}As_2$ samples were prepared from stoichiometric mixtures of Ba, K, and $Fe_{0.93}Co_{0.07}As$ in alumina crucibles, sealed in silica tubes, and heated to 640 °C. The samples were homogenized and annealed at 710–790 °C several times. Resistivities were measured with cold pressed and annealed (500–600 °C) pellets using the four-probe method. Bulk superconductivity was confirmed by AC susceptibility measurements. Powder diffraction data were measured using a Huber G670 diffractometer (Co $K_{\alpha 1}$ or Cu $K_{\alpha 1}$ radiation), equipped with a closed-cycle He cryostat. Rietveld refinements were performed with the TOPAS package using the fundamental parameter approach and an empirical $2\theta$-dependent intensity correction for Guinier geometry. The Fe:Co ratio was held constant and the Ba:K ratios were refined. The results agree well with EDX measurements with potassium content variations by no more than ±4% and variations of the Co content by no more than ±1%. $^{57}$Fe Mössbauer spectra of $Ba_{0.8}K_{0.2}Fe_{1.86}Co_{0.14}As_2$ were recorded in transmission geometry using a $^{57}$Co/Rh source. The spectrometer was calibrated with a 8 μm thin α-Fe foil.

Received: April 26, 2011
Published online: June 29, 2011

**Keywords:** iron arsenides · magnetic properties · phase diagrams · solid-state structures · superconductivity

[1] Y. Kamihara, T. Watanabe, M. Hirano, H. Hosono, *J. Am. Chem. Soc.* **2008**, *130*, 3296.
[2] Z.-A. Ren, W. Lu, J. Yang, W. Yi, X.-L. Shen, Z.-C. Li, G.-C. Che, X.-L. Dong, L.-L. Sun, F. Zhou, Z.-X. Zhao, *Chin. Phys. Lett.* **2008**, *25*, 2215.
[3] M. Rotter, M. Tegel, D. Johrendt, *Phys. Rev. Lett.* **2008**, *101*, 107006.
[4] S. Medvedev, T. M. McQueen, I. A. Troyan, T. Palasyuk, M. I. Eremets, R. J. Cava, S. Naghavi, F. Casper, V. Ksenofontov, G. Wortmann, C. Felser, *Nat. Mater.* **2009**, *8*, 630.
[5] D. C. Johnston, *Adv. Phys.* **2010**, *59*, 803.
[6] R. Pöttgen, D. Johrendt, *Z. Naturforsch. B* **2008**, *63*, 1135.
[7] Y. Kamihara, H. Hiramatsu, M. Hirano, R. Kawamura, H. Yanagi, T. Kamiya, H. Hosono, *J. Am. Chem. Soc.* **2006**, *128*, 10012.
[8] M. J. Pitcher, D. R. Parker, P. Adamson, S. J. C. Herkelrath, A. T. Boothroyd, R. M. Ibberson, M. Brunelli, S. J. Clarke, *Chem. Commun.* **2008**, 5918.
[9] F. C. Hsu, J. Y. Luo, K. W. Yeh, T. K. Chen, T. W. Huang, P. M. Wu, Y. C. Lee, Y. L. Huang, Y. Y. Chu, D. C. Yan, M. K. Wu, *Proc. Natl. Acad. Sci. USA* **2008**, *105*, 14262.
[10] C. de La Cruz, Q. Huang, J. W. Lynn, J. Y. Li, W. Ratcliff, J. L. Zarestky, H. A. Mook, G. F. Chen, J. L. Luo, N. L. Wang, P. C. Dai, *Nature* **2008**, *453*, 899.
[11] H. H. Klauss, H. Luetkens, R. Klingeler, C. Hess, F. J. Litterst, M. Kraken, M. M. Korshunov, I. Eremin, S. L. Drechsler, R. Khasanov, A. Amato, J. Hamann-Borrero, N. Leps, A. Kondrat, G. Behr, J. Werner, B. Büchner, *Phys. Rev. Lett.* **2008**, *101*, 077005.
[12] M. Rotter, M. Tegel, I. Schellenberg, W. Hermes, R. Pöttgen, D. Johrendt, *Phys. Rev. B* **2008**, *78*, 020503.
[13] D. R. Parker, M. J. Pitcher, P. J. Baker, I. Franke, T. Lancaster, S. J. Blundell, S. J. Clarke, *Chem. Commun.* **2009**, 2189.
[14] I. I. Mazin, *Nature* **2010**, *464*, 183.
[15] I. Mazin, *Physics* **2011**, *4*, 26.
[16] J. Dong, H. J. Zhang, G. Xu, Z. Li, G. Li, W. Z. Hu, D. Wu, G. F. Chen, X. Dai, J. L. Luo, Z. Fang, N. L. Wang, *arXiv:* 0803.3426.
[17] A. D. Christianson, E. A. Goremychkin, R. Osborn, S. Rosenkranz, M. D. Lumsden, C. D. Malliakas, I. S. Todorov, H. Claus, D. Y. Chung, M. G. Kanatzidis, R. I. Bewley, T. Guidi, *Nature* **2008**, *456*, 930.
[18] H. Ding, P. Richard, K. Nakayama, K. Sugawara, T. Arakane, Y. Sekiba, A. Takayama, S. Souma, T. Sato, T. Takahashi, Z. Wang, X. Dai, Z. Fang, G. F. Chen, J. L. Luo, N. L. Wang, *Epl* **2008**, *83*, 47001.
[19] I. I. Mazin, D. J. Singh, M. D. Johannes, M. H. Du, *Phys. Rev. Lett.* **2008**, *101*, 057003.
[20] K. Kuroki, S. Onari, R. Arita, H. Usui, Y. Tanaka, H. Kontani, H. Aoki, *Phys. Rev. Lett.* **2008**, *101*, 087004.
[21] Y.-Z. Zhang, I. Opahle, H. O. Jeschke, R. Valenti, *Phys. Rev. B* **2010**, *81*, 094505.
[22] M. Rotter, M. Pangerl, M. Tegel, D. Johrendt, *Angew. Chem.* **2008**, *120*, 8067; *Angew. Chem. Int. Ed.* **2008**, *47*, 7949.
[23] A. S. Sefat, R. Jin, M. A. McGuire, B. C. Sales, D. J. Singh, D. Mandrus, *Phys. Rev. Lett.* **2008**, *101*, 117004.
[24] S. Drotziger, P. Schweiss, K. Grube, T. Wolf, P. Adelmann, C. Meingast, H. v. Löhneysen, *J. Phys. Soc. Jpn.* **2010**, *79*, 124705.
[25] H. Wadati, I. Elfimov, G. A. Sawatzky, *Phys. Rev. Lett.* **2010**, *105*, 157004.
[26] M. Neupane, P. Richard, Y. M. Xu, K. Nakayama, T. Sato, T. Takahashi, A. V. Federov, G. Xu, X. Dai, Z. Fang, Z. Wang, G. F. Chen, N. L. Wang, H. H. Wen, H. Ding, *Phys. Rev. B* **2011**, *83*, 094522.

  

[27] A. S. Sefat, D. J. Singh, L. H. VanBebber, Y. Mozharivskyj, M. A. McGuire, R. Jin, B. C. Sales, V. Keppens, D. Mandrus, *Phys. Rev. B* **2009**, *79*, 224524.
[28] Y. Muraba, S. Matsuishi, S.-W. Kim, T. Atou, O. Fukunaga, H. Hosono, *Phys. Rev. B* **2010**, *82*, 180512.
[29] A. Jesche, N. Caroca-Canales, H. Rosner, H. Borrmann, A. Ormeci, D. Kasinathan, H. H. Klauss, H. Luetkens, R. Khasanov, A. Amato, A. Hoser, K. Kaneko, C. Krellner, C. Geibel, *Phys. Rev. B* **2008**, *78*, 452201.
[30] S. Suzuki, K. Ohgushi, Y. Kiuchi, Y. Ueda, *Phys. Rev. B* **2010**, *82*, 184510.
[31] C. H. Lee, A. Iyo, H. Eisaki, H. Kito, M. T. Fernandez-Diaz, T. Ito, K. Kihou, H. Matsuhata, M. Braden, K. Yamada, *J. Phys. Soc. Jpn.* **2008**, *77*, 083704.
[32] R. Cortes-Gil, D. R. Parker, M. J. Pitcher, J. Hadermann, S. J. Clarke, *Chem. Mater.* **2010**, *22*, 4304.

  